JOURNAL OF COMPUTATIONAL PHYSICS 71, 147–168 (1987)

Fronts, Relaxation Oscillations, and Period Doubling in Solid Fuel Combustion*

A. BAYLISS†

EXXON Corporate Research Science Laboratories,
EXXON Research and Engineering Company,
Clinton Township, Route 22 East, Annandale, New Jersey 08801

AND

B. J. MATKOWSKY

Department of Engineering Sciences and Applied Mathematics,
The Technological Institute, Northwestern University, Evanston, Illinois 60201

Received June 2, 1986; Revised September 19, 1986

We consider a reaction–diffusion system which models the gasless combustion of a solid material. The system exhibits oscillating fronts, whose nature varies as a function of the parameters of the problem. The behavior of the solution along the bifurcation branches is studied numerically, by an adaptive Chebychev pseudo-spectral method in which the coordinate system is adapted to follow the sharp oscillations of the front. As the bifurcation parameter is increased through a primary bifurcation point, the solution exhibits a transition from a steadily propagating front to a sinusoidally oscillating front. This front develops into a relaxation oscillation whose peaks become progressively sharper and steeper. As a secondary bifurcation point is exceeded, a period-doubling bifurcation occurs.

INTRODUCTION

In this paper we consider a system of reaction–diffusion equations which describe gasless, condensed phase or solid fuel combustion. In this type of combustion, the chemical reaction takes place in the solid fuel itself, which is transformed directly into solid combustion products without any gas phase formation. Condensed phase combustion is currently being studied as a new and potentially more effective means of synthesizing ceramic and metallic materials which have, e.g., greater tolerances to high temperature and superior mechanical and electrical characteristics. Due to the exothermic chemical reaction, a temperature front propagates from the high tem-

* This research was supported in part by the U.S. Department of Energy under Grant DE FGO2-87ER25027

† Present address: Department of Engineering Sciences and Applied Mathematics, The Technological Institute, Northwestern University, Evanston, IL 60201

0021-9991/87 $3.00

perature combustion products, to the low temperature unburned fuel. Previous results, both theoretical and experimental, have indicated that various modes of propagation are possible. In addition to uniformly propagating planar fronts, experimenters [1–4] also observed planar fronts whose propagation velocities are oscillatory in time, referred to as self-oscillatory combustion. Other modes of propagation, including spin combustion, in which a spiraling motion of a non-uniform front (one or more luminous points move in a helical fashion along the surface of a cylindrical sample) have also been observed.

A theoretical analysis of the one-dimensional case was undertaken by Matkowsky and Sivashinsky [5] who showed that the self-oscillatory mode arose as a Hopf bifurcation from the uniformly propagating planar front, as a critical parameter μ_c, of the system, was exceeded. The parameter μ was identified as the product of a nondimensional activation energy energy of the reaction, and a factor measuring the difference between the nondimensionalized temperatures of the unburned fuel and the combustion products.

Matkowsky and Sivashinsky showed that the uniformly propagating planar front is stable for $\mu < \mu_c$. For $\mu > \mu_c$, they showed that the uniform front is unstable and perturbations evolve to the bifurcated state, i.e., to the pulsating propagating state. In their bifurcation analysis, they calculated the amplitude, frequency and velocity of the pulsating front. Such an analysis is necessarily valid only locally, in a neighborhood of the bifurcation point. To determine more global behavior, i.e., to determine the behavior of the system beyond this neighborhood, it is necessary to determine the bifurcation branch(es) numerically. To do so, we introduce an adaptive pseudo-spectral method for the numerical solution of the one-dimensional problem. Employing this method we are able to show how the sinusoidal oscillations predicted by bifurcation theory develop into relaxation oscillations as we proceed to higher values of μ. Finally, we are able to numerically identify a period doubling secondary bifurcation. The oscillations in the velocity exhibit sharp narrow spikes alternating with longer slowly varying behavior. The peaks of the oscillations become progressively sharper and steeper as μ is increased. This behavior makes adaptive techniques particularly attractive.

In our approach, we solve the problem as an initial boundary value problem, integrating in time until a stable oscillatory steady state is achieved. Thus we necessarily compute only the stable branches of the bifurcation diagram. Generally the solution reaches its steady state after a relatively short period of time, except near bifurcation points where much longer times are required to reach steady state conditions.

We introduce an adaptive Chebychev pseudo-spectral method for the numerical discretization of the partial differential equations. The standard Chebychev method (see, e.g., Gottlieb and Orszag [6]) is modified to adaptively adjust the coordinate system, as the solution evolves in time. New coordinate systems are generated by an explicit transformation which is chosen so that a Sobolev-type semi-norm is minimized in the new coordinate system. In this way the spatial discretization error is reduced and the efficiency of the pseudo-spectral method is enhanced.

Relaxation oscillations have been found numerically for problems involving ordinary differential equations (see, e.g., [7, 8] who employed an idea of [9]). Rogg [10] and Smooke and Koszykowski [11] found examples of relaxation oscillations for one dimensional problems in gaseous combustion by employing a method of lines, followed by an ODE solver in time, and an adaptive finite difference scheme, respectively. Margolis [12], employing a spline collocation method, found an example of a doubly periodic relaxation oscillation for a one-dimensional burner stabilized gaseous combustion problem. However, the mechanism by which the doubly periodic oscillation was generated, i.e., by secondary bifurcation, was not determined. Finally, Baer and Erneux [13] analytically described the development of relaxation oscillations from sinusoidal oscillations, for a class of ordinary differential equations characterized by two time scales.

In Section 2 we introduce the mathematical model. In Section 3 we describe the numerical method including a brief description of the standard Chebychev pseudo-spectral method and our adaptive Chebychev pseudo-spectral method as well as details regarding its implementation. Our results appear in Section 4, and Section 5 is a summary and conclusion section.

2. Mathematical Model

In this section we briefly discuss the mathematical model. We employ a generalization of the models employed in [5, 14], in which the effect of melting of one of the reactants is taken into account, and in which the reaction is cut off in the solid unburned fuel. Assuming the front propagates in the $\tilde{x}$ direction, we let $\tilde{x}=\tilde{\phi}(\tilde{t})$ denote the position of the melting front at time $\tilde{t}$. If $\tilde{T}$ and $\tilde{C}$ denote the temperature, and the concentration of the limiting component of the reaction, respectivly, the model is described by the reaction–diffusion system

$$\begin{aligned}\tilde{T}_{\tilde{t}} &= \tilde{\lambda}\tilde{T}_{\tilde{x}\tilde{x}} + \begin{pmatrix}\tilde{\beta}\\ \alpha(\tilde{\beta}+\tilde{\gamma})\end{pmatrix} g\tilde{A}\tilde{C}\exp(-\tilde{E}/R\tilde{T})\\ \tilde{C}_{\tilde{t}} &= -\begin{pmatrix}1\\ \alpha\end{pmatrix} g\tilde{A}\tilde{C}\exp(-\tilde{E}/R\tilde{T}),\end{aligned} \tag{2.1}$$

where

$$\begin{pmatrix}a\\ b\end{pmatrix} = \begin{cases}a, & \tilde{x}<\tilde{\phi}(\tilde{t})\\ b, & \tilde{x}>\tilde{\phi}(\tilde{t}).\end{cases}$$

Here $\tilde{\lambda}$ denotes the thermal conductivity, $\tilde{A}$ is the rate constant and $\tilde{\beta}$ the heat of reaction. Because of melting, the rate constant is amplified by the constant $\alpha>1$, due to the increased surface to surface contact of the reactants. Upon melting the heat of fusion $\tilde{\gamma}$ is absorbed by the material, but is then released during the reaction process so that the product is in the solid phase. Thus behind the melting surface,

the heat of reaction is augmented by $\tilde{\gamma}$. $\tilde{E}$ denotes the activation energy and R the gas constant. Finally the function

$$g = g(\tilde{x} - \tilde{\phi}(\tilde{t})) = \begin{cases} 1, & \tilde{x} - \tilde{\phi}(\tilde{t}) > z_c \\ 0, & \tilde{x} - \tilde{\phi}(\tilde{t}) < z_c \end{cases}$$

is introduced to cut off the reaction in the unburned region, to model the fact that the reaction does not occur significantly before melting. We will discuss the sensitivity of our results to the specific choice of the constant z_c and to the form of the cut off function, below.

Across the melting surface there is a jump in the heat flux, due to the absorption of the heat of fusion necessary to cause melting. The velocity $\tilde{\phi}_{\tilde{t}}$ of the melting surface satisfies

$$\tilde{\phi}_{\tilde{t}} = -\frac{\tilde{\lambda}}{\tilde{\gamma}\tilde{C}_m}[\tilde{T}_{\tilde{x}}], \tag{2.2}$$

where C_m is the concentration at the melting surface and $[\tilde{T}_{\tilde{x}}]$ denotes the jump in $\tilde{T}_{\tilde{x}}$ across this surface. The boundary conditions for the system are given by

$$\begin{aligned} &\tilde{C} \to \tilde{C}_u, \qquad \tilde{T} \to \tilde{T}_u, \qquad \text{as} \quad \tilde{x} \to -\infty \\ &\tilde{C} \to 0, \qquad \tilde{T} \to \tilde{T}_b \qquad \text{as} \quad \tilde{x} \to +\infty, \end{aligned} \tag{2.3}$$

where the subscripts u and b refer to unburned and burned, respectively. We observe that the burned temperature $\tilde{T}_b$ is derivable from the time-independent solution of the problem as $\tilde{T}_b = \tilde{T}_u + \tilde{\beta}\tilde{C}_u$.

We nondimensionalize by introducing

$$\begin{aligned} &C = \frac{\tilde{C}}{\tilde{C}_u}, \qquad \theta = \frac{\tilde{T} - \tilde{T}_u}{\tilde{T}_b - \tilde{T}_u}, \qquad t = \frac{\tilde{t}\tilde{U}^2}{\tilde{\lambda}}, \qquad x = \frac{\tilde{x}\tilde{U}}{\tilde{\lambda}}, \\ &\phi = \frac{\tilde{\phi}\tilde{U}}{\tilde{\lambda}}, \qquad \sigma = \frac{\tilde{T}_u}{\tilde{T}_b}, \qquad \gamma = \frac{\tilde{\gamma}}{\tilde{\beta}}, \qquad N = \frac{\tilde{E}}{R\tilde{T}_b}. \end{aligned} \tag{2.4}$$

The reference velocity $\tilde{U}$ is the velocity of the uniformly propagating front in the asymptotic limit $N \gg 1$. We also introduce the moving coordinate system

$$z = x - \phi(t) \tag{2.5}$$

so that the position of the melting front is fixed at $z = 0$.

In terms of the nondimensionalized quantities, and the transformation (2.5), the system (2.1) becomes

$$\begin{aligned} \theta_t &= \phi_t \theta_z + \theta_{zz} + \begin{pmatrix} I \\ \alpha(1+\gamma) \end{pmatrix} g(z)\, \Lambda C \exp\left(\frac{N(1-\sigma)(\theta-1)}{\sigma + (1-\sigma)\theta}\right) \\ C_t &= \phi_t C_z - \begin{pmatrix} 1 \\ \alpha \end{pmatrix} g(z)\, \Lambda C \exp\left(\frac{N(1-\sigma)(\theta-1)}{\sigma + (1-\sigma)\theta}\right) \end{aligned} \tag{2.6}$$

subject to the boundary conditions

$$\begin{aligned} C &\to 1, \qquad \theta \to 0 \quad \text{as} \quad z \to -\infty \\ C &\to 0, \qquad \theta \to 1 \quad \text{as} \quad z \to +\infty. \end{aligned} \tag{2.7}$$

Note that the boundary condition $C \to 0$ as $z \to +\infty$, follows from (2.6). At the melting surface $z = 0$, the temperature θ is fixed at θ_m, and the velocity of the surface is obtained from

$$[\theta_z] + \gamma C(0)\, \phi_t = 0. \tag{2.8}$$

The quantity $A = (\tilde{\lambda}\tilde{A}/\tilde{U}^2)\exp(-\tilde{E}/R\tilde{T}_b)$ is unknown, and depends on the (unknown) velocity $\tilde{U}$. It can be determined by finding the solution corresponding to the steadily propagating front. An asymptotic ($N \gg 1$) expression for A was derived in [14]. For our purposes, however, it is not necessary to find A, since a particular choice of A merely corresponds to a specific choice of length and time scales, and thus does not affect the properties of the oscillatory solutions.

We note that the solution of our problem will be shown to exhibit bifurcation phenomena as the parameter $\mu = A/2(1-M)$, where $A = N(1-\sigma)$ and

$$M = \left(1 - \frac{(1+\gamma)}{\alpha}\right) e^{A(\theta_m - 1)},$$

is varied.

In order to have a model which is amenable to numerical computation, it is necessary to reduce the problem defined on the infinite domain, to one on a finite domain (z_L, z_R). Thus we actually employ the boundary conditions

$$C(z_L) = 1, \qquad \theta(z_L) = 0, \qquad \theta(z_R) = 1. \tag{2.9}$$

Below we will discuss the sensitivity of the computation to the choice of z_L and z_R.

3. Numerical Method

In this section we discuss the numerical method. The section is divided into three subsections. In A we give a brief description of the standard Chebychev pseudo-spectral method. In B we describe our adaptive algorithm, while in C we describe details of the implementation which are specific to the problem described above.

3A. *Standard Pseudo-spectral Algorithm*

An extensive description of the well-known Chebychev pseudo-spectral method may be found in [6]. The brief description that follows is presented only to make the paper self-contained. To illustrate the method we consider the model equation

$$u_t = au_{xx} + bu_x, \qquad -1 \leqslant x \leqslant 1. \tag{3.1}$$

We assume that $u(x, t)$ can be expanded as a finite sum of Chebychev polynomials as

$$u(x, t) = \sum_{n=0}^{J} a_n(t)\, T_n(x), \tag{3.2}$$

where

$$T_n(x) = \cos(n \cos^{-1} x)$$

is the nth Chebychev polynomial. The coefficients $a_n(t)$ are determined by requiring (3.2) to exactly solve (3.1) at a set of collocation points $\{x_j;\ j = 0, 1, \ldots, J\}$. The standard collocation sequence is given by

$$x_j = \cos\frac{j\pi}{J}, \qquad j = 0, 1, \ldots, J. \tag{3.3}$$

Substituting (3.2) into (3.1), we obtain

$$u_t(x_j, t) = a \sum_{n=0}^{J} a_n(t)\, T_n''(x_j) + b \sum_{n=0}^{J} a_n(t)\, T_n'(x_j). \tag{3.4}$$

The functions $T_n'(x)$ and $T_n''(x)$ can be related to $T_n(x)$ by well-known recursion relations [6], and (3.4) can be rewritten as

$$u_t(x_j, t) = \sum_{n=0}^{J} b_n(t)\, T_n(x_j), \tag{3.5}$$

where the sequence $\{b_n\}$ is determined by $\{a_n\}$, a, b, and the recursion relation. Finally, using the definition of T_n and (3.3), (3.5) can be written as

$$u_t(x_j, t) = \sum_{n=0}^{J} b_n \cos\frac{nj\pi}{J} = F(u(x_1, t), u(x_2, t), \ldots, u(x_J, t)). \tag{3.6}$$

This system can now be solved by advancing the solution in time at the nodal points. Thus the Chebychev pseudo-spectral method can be implemented by one FFT to obtain $\{a_n\}$ from $\{u(x_j, t)\}$, a recursion to obtain $\{b_n\}$ from $\{a_n\}$, and another FFT to obtain $\{u_x(x_j, t)\}$ from $\{b_n\}$. Alternatively we can construct a matrix which directly relates $\{u_x(x_j, t)\}$ to $\{u(x_j, t)\}$. The former implemention asymptotically requires $O(J \log J)$ operations, while the latter requires $O(J^2)$ operations. Nevertheless, on vector computers, for certain J, it may be more efficient to employ the latter implementation. Clearly the choice of which implementation to use depends on J, on the specific FFT employed and on the computer architecture.

The method described above is a global method, using data at all points $\{x_j\}$ to compute u_x at any collocation point. This is in contrast to finite difference schemes,

which are local. It is known that for smooth functions, pseudo-spectral methods converge faster than $O(J^{-r})$ for any $r>0$, in contrast to finite difference methods which converge as $O(n^{-r})$ for r fixed, e.g., 2 or 4, where n is the number of grid points. Finally, the pseudo-spectral method maintains spectral accuracy up to the boundaries, in contrast to finite difference methods which require special treatment near boundaries.

3B. *Adaptive Pseudo-spectral Algorithm*

The polynomial obtained from collocating at the sequence of points (3.3) is not in general the optimal interpolation for all functions u. It is well known that the optimal (in any given norm) sequence of interpolation points depends on the function itself [15]. Intuitively it would be expected that for solutions with steep gradients which propagate in time, the deviation of (3.3) from the optimal collocation points will be strongly time-dependent. In this section we consider an algorithm to dynamically vary the collocation points according to properties of the solution as it evolves.

Let I denote the interval $[-1, 1]$. Consider the model equation

$$u_t = au_{xx} + bu_x, \qquad x \in I. \tag{3.7}$$

Let $q(s, \boldsymbol{\alpha})$ be a function such that for each value of the parameter vector $\boldsymbol{\alpha}$, $q(\cdot, \boldsymbol{\alpha})$ is a univalent mapping of I onto itself. A specified functional form for q will be introduced below. The mapping

$$x = q(s, \boldsymbol{\alpha}) \tag{3.8}$$

defines a family of coordinate systems which depend on $\boldsymbol{\alpha}$. Under the transformation (3.8), (3.7) becomes

$$u_t = a\left(\frac{u_{ss}}{q'^2} - \frac{u_s q''}{q'^3}\right) + b\frac{u_s}{q'}. \tag{3.9}$$

We observe that the Chebychev pseudo-spectral method can be applied to (3.9) for any value of $\boldsymbol{\alpha}$.

For any function $v(x)$, any weight function $w(x)>0$, and integer $K \geqslant 0$ we define

$$\|v\|^2_{K,w} = \sum_{j=0}^{K} \int_{-1}^{1} |v^j|^2 w(x)\, dx. \tag{3.10}$$

When $K=0$, (3.10) is the L_2 norm with weight $w(x)$. Let $e_J = v - v_J$ denote the spectral interpolation error, where v_J is the interpolant of v at the collocation sequence (3.3). It is shown in [16] that for $0 \leqslant i \leqslant K$

$$\|e_n\|_{i,w} \leqslant CJ^{2i-r}\|v\|_{r,w}, \tag{3.11}$$

where C is a constant and $w(x)$ is the Chebychev weight function

$$w(x) = (1 - x^2)^{-1/2}.$$

A similar estimate was proved in [17] for the error in approximating a model (hyperbolic) initial boundary value problem by the Chebychev pseudo-spectral method.

The estimate (3.11) indicates that the spectral interpolation error, which is one of the components of the error in the Chebychev pseudo-spectral method can be reduced by working in a coordinate system in which some Sobolev-type semi-norm of the solution is reduced. This is the basis for our adaptive algorithm.

Specifically suppose that at a given time t_1, $u(x, t_1)$ is an approximate solution of (3.7). For any coordinate system defined by $\boldsymbol{\alpha}$, let

$$I(\boldsymbol{\alpha}) = \int_{-1}^{1} w(s)[A|u_{ss}|^2 + B|u_s|^2 + C|u|^2]\, ds. \tag{3.12}$$

In the original (x) coordinate system (3.12) can be rewritten as

$$I(\boldsymbol{\alpha}) = \int dx\, s_x w(s(x, \boldsymbol{\alpha}))[A|u_{xx}x_s^2 + u_x x_{ss}|^2 + B|u_x u_s|^2 + C|u|^2]. \tag{3.13}$$

In (3.13) $s(x, \boldsymbol{\alpha})$ is the inverse of the mapping $x = q(s, \boldsymbol{\alpha})$ and x_s and x_{ss} can be evaluated as functions of x and $\boldsymbol{\alpha}$ by explicit differentiation. We will choose $\boldsymbol{\alpha}$, which defines the new coordinate system, by minimizing the functional $I(\boldsymbol{\alpha})$. In practice, we add a penalty to $I(\boldsymbol{\alpha})$ in order to prevent the Jacobian of the mapping from becoming too large. Specifically we add to $I(\boldsymbol{\alpha})$ the term $s_x(x_0, \boldsymbol{\alpha})$, where x_0 is a fixed point (corresponding to the melting front in the application considered here). This prevents too many points from piling up near the front, with too few points included in the regions away from the front. Once a new coordinate system is determined, the solution is interpolated to the Chebychev collocation sequence (3.3) in the new coordinate system by using the global expansion (3.2).

We now describe the adaptive algorithm:

(i) integrate to $t = t_1$ in an initial coordinate system,

(ii) find $\boldsymbol{\alpha}_{\min}$ which minimizes $I(\boldsymbol{\alpha})$,

(iii) interpolate the solution to the Chebychev points in the new coordinate system by evaluating the Chebychev interpolant,

(iv) integrate to $t = t_2$,

(v) go to (ii).

The times $t_1, t_2, \ldots$ for which a new coordinate system is computed, can be chosen dynamically. We can trigger a search for a new coordinate system when some

functional monitoring the solution, changes by more than a prescribed amount from the previous time a coordinate system was found. For the problem considered here we have used both $|\phi_t|$ and $I(\boldsymbol{\alpha})$. Monitoring changes in $I(\boldsymbol{\alpha})$ is applicable to more general problems, e.g., gaseous combustion problems where the analog of a melting front does not exist.

In practice we input two constants $c_1 < 1$ and $c_2 > 1$ and do not adapt as long as the inequality

$$c_1 < \frac{I(\boldsymbol{\alpha}_{\min})}{\tilde{I}} < c_2$$

is satisfied. Here $\tilde{I}$ is the value of the functional I the last time a coordinate system was found. Values of $c_1 \sim 0.7$ and $c_2 \sim 1.4$ appear to be satisfactory. One can also adapt at specified time intervals.

We have found that in practice several hundred time steps will occur before another search is required. Therefore the additional computer time required for the adaptive procedure is very small. The previous value of $\boldsymbol{\alpha}$ is a very good guess for the new value of $\boldsymbol{\alpha}$. A Gauss–Chebychev quadrature formula is used to compute the integrals in (3.12).

Since the interpolation is done using the global Chebychev expansion the entire process preserves the spectral accuracy. It is known that the Chebychev interpolant can exhibit oscillations [6], due to the Gibbs phenomenon. In order to use the Chebychev interpolant to interpolate to the new collocation points, it is necessary to be certain that the interpolant is free of oscillations. For the problems considered here, this is in fact true. One reason is that the adaptive algorithm is designed to use coordinate systems in which the solution does not exhibit steep gradients. Of course other interpolation formulae could be used as well.

It has been observed (see, e.g., [6] and [18]) that the Chebychev pseudo-spectral method can be quite inaccurate when J is too small. As J increases beyond a critical value there is an abrupt decrease in the error and the computed solution becomes extremely accurate. Further increasing J does not lead to significantly greater accuracy. This is in contrast to finite differences where the errors change much more gradually as the number of grid point changes. For this reason the results of the adaptive pseudo-spectral algorithm may be considerably more dramatic than for adaptive finite difference methods.

As the coordinate system is changed the clustering of the collocation points changes. It is conjectured that the convection time-step restriction can be related to the smallest distance between the collocation points [6], although the Chebychev method is a global method and standard domain of dependence arguments are not valid. Employing this relationship, the time step can also be changed adaptively together with the coordinate system.

A higher-dimensional extension of the method appears to be quite feasible, using any one of a number of existing programs which map the square onto itself; or alternatively by extending the mapping described below, to two dimensions.

3C. *Details of the Implementation*

In this subsection we briefly outline some details of the implementation of the algorithm that are particular to the model described in Section 2. We first discuss the time differencing.

Consider the model equation

$$u_t = u_{xx} + Bu_x + R(u). \tag{3.14}$$

Here the coefficient B of the first derivative is a functional of u which corresponds to the front velocity ϕ_t in our problem. It will be seen in the next section that ϕ_t may be a rapidly varying function in time. ϕ_t also depends on the solution in a

Specifically, assume the solution is known at time level n. We make a prediction at time level $n+\frac{1}{2}$,

$$u^{n+1/2} = u^n + \frac{\Delta t}{2} u_{xx}^{n+1/2} + \frac{\Delta t}{2}(B^n u_x^n + R(u^n)) \tag{3.15}$$

and a correction to obtain u^{n+1},

$$u^{n+1} = u^n + \frac{\Delta t}{2}(u_{xx}^{n+1} + u_{xx}^n) + \Delta t\,(B^{n+1/2} u_x^{n+1/2} + R(u^{n+1/2})). \tag{3.16}$$

After the prediction (3.15), the front velocity (i.e., $B^{n+1/2}$) is computed from its definition, and then employed in (3.16). The scheme (3.15), (3.16) is second-order accurate. In practice we solve the transformed equation (3.9). The matrix associated with the semi-implicit scheme (3.15) (or (3.16)) is factored each time a new coordinate system is computed.

The time-step is limited by the convective stability condition which is discussed in [6]. The time-step is adaptively changed as the coordinate system is adapted and as ϕ_t changes. Specifically if d_α is the smallest distance between the collocation points in the coordinate system α, we assume

$$\Delta t \simeq \frac{\kappa}{|B^n d_\alpha|}. \tag{3.17}$$

The assumption (3.17) has not been shown rigorously, but we have found that this is the time-step restriction for the adaptive algorithm employed on our model. In practice we require $\kappa \simeq 0.7$ for 1% errors due to the time differencing. Thus the time-step is limited by accuracy constraints rather than by stability.

We use a coordinate transformation of the form

$$q(s, \boldsymbol{\alpha}) = \frac{4}{\pi} \tan^{-1} \alpha_1 \tan\left(\frac{\pi}{4}(s' - 1)\right) + 1$$

$$s' = \frac{\alpha_2 - s}{\alpha_2 s - 1} \tag{3.18}$$

$$\alpha_1 > 0, \qquad -1 < \alpha_2 < 1, \qquad s \in I.$$

Other choices of q are possible.

In the functional (3.13) the constants A, B, and C were chosen to be $A = B = 1$, $C = 0$. These values were not changed for any of the cases considered. Clearly other choices are possible. Though we tested both the Chebychev weight function $w = (1 - x^2)^{-1/2}$ and the weight factor $w = 1$, the results did not seem to vary significantly. The results presented below all correspond to the Chebychev weight function. In practice the adaption is done only in the region behind the front since the solution changes much more rapidly in this region, and adaption does not appear to be necessary ahead of the front. In the functional I, only the nondimensional temperature θ, and not the concentration C, is employed.

4. Results

The results we present are designed to both demonstrate the effectiveness of our adaptive method and to illustrate the behavior of the solution beyond the neighborhood of the first bifurcation point, where analytical results are available. Throughout this section we employ the parameter values: $N = 50$, $\alpha \approx 1.7$, $\gamma = 0.5$, $\theta_m = 0.8$. The bifurcation parameter μ is varied by varying the temperature ratio σ.

4A. *Effectiveness of Adaptive Algorithm*

We first consider one specific case in order to demonstrate the effectiveness of the adaptive algorithm. Thus we consider the problem with $\mu = 4.3679$, corresponding to $\sigma = 0.829$. We apply the boundary condition (2.9) at $z_R = -z_L = 8$. In addition we take $g = 1$, which is equivalent to cutting off the reaction beyond z_L, i.e., not cutting it off in the computational domain. These results are typical of results where the reaction is cut off within the computational domain. The stable solution is oscillatory and has begun to exhibit spikes. In the computation, we use the same number of collocation points on both sides of the melting front. The adaptive procedure is applied only behind the melting front, where temperature spikes occur.

In Fig. 1 the front velocity is shown for n (the number of collocation points on each side of the melting front) varying from 17 to 65. The adaptive algorithm was not used, so that the standard collocation points are employed. It is apparent that the solutions obtained with $n = 17$, 25, and 33 are inaccurate. The agreement

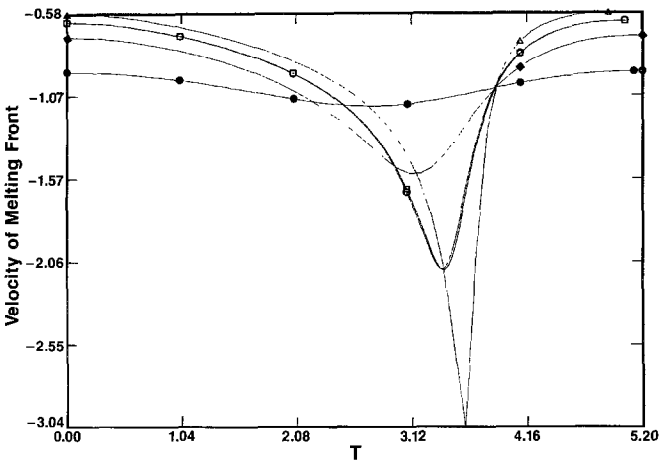

FIG. 1. Velocity of the melting front for different numbers of collocation points. The adaptive algorithm is not used. $\mu = 4.368$; □, $n = 65$; ○, $n = 49$; △, $n = 33$, ◆, $n = 25$; ●, $n = 17$.

between the solutions obtained with $n = 49$ and $n = 65$ is an example of the abrupt change in the convergence of the Chebychev pseudo-spectral method, once sufficient resolution is achieved, and that additional resolution provides no significant improvement in accuracy.

In Fig. 2 we show the front velocity obtained by using the adaptive algorithm. The improvement in accuracy for the coarse grids is apparent. As a further verification of the numerical algorithm we plot in Figs. 3 and 4 the normalized temperature $\theta(z)$. The profile is shown at the time corresponding to the spike in the

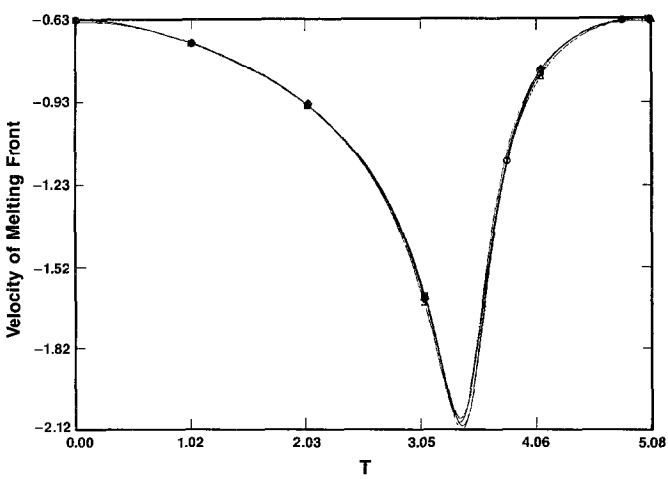

FIG. 2. Velocity of the melting front. Coarse grids ($n = 17$, 25, and 33) are computed using the adaptive algorithm. The fine grid, $n = 65$, is computed without using the adaptive algorithm. $\mu = 4.368$; □, $n = 65$, ○, $n = 33$; △, $n = 25$; ◆, $n = 17$.

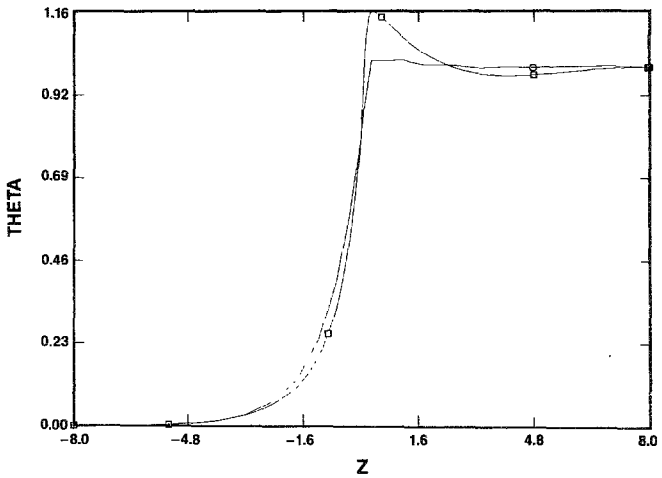

FIG. 3. Temperature profile, $\theta(z)$, at the instant that the velocity of the melting front spikes. Computations with $n = 65$ and $n = 17$ are compared. The adaptive algorithm is not used. $\mu = 4.368$; □, $n = 65$; ○, $n = 17$.

front velocity. In Fig. 3 we plot $\theta(z)$ for $n = 17$, and $n = 65$ without using the adaptive algorithm. In Fig. 4 we show $\theta(z)$ for $n = 17$ (adaptive) and $n = 65$ (non-adaptive). The improvement in accuracy is again apparent.

The results above demonstrate the effectiveness of the adaptive algorithm on this class of problems. We also point out that the steady oscillations obtained with the adaptive algorithm are insensitive to the choice of initial conditions. As an experiment we started with the smooth (but erroneous) solution obtained with

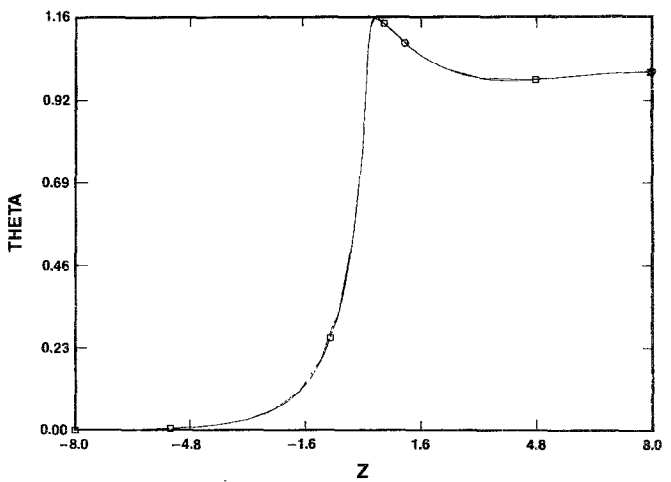

FIG. 4. Temperature profile, $\theta(z)$ at the instant that the velocity of the melting front spikes. Computations with $n = 17$ (adaptive) and $n = 65$ (non-adaptive) are compared. $\mu = 4{,}368$; □, $n = 65$; ○, $n = 17$.

$n = 25$ and without using the adaptive algorithm. After switching on the adaptive algorithm and allowing the transient to decay, the solution displayed in figure 2 was obtained.

4B. *The Solution beyond the First Bifurcation Point*

We consider the model with $z_c = -3$, i.e., the reaction terms are abruptly cut off 3 units ahead of the melting front. We have verified that the solutions are insensitive to the particular form of the cut off function, and are relatively insensitive to the position of the cut off in the range $-5 \leqslant z_c \leqslant -2$, i.e., anywhere from about 15% to more than 40% of the computation domain. For a wider range of cut-off locations, the solution does change somewhat. For a fixed value of μ, moving the

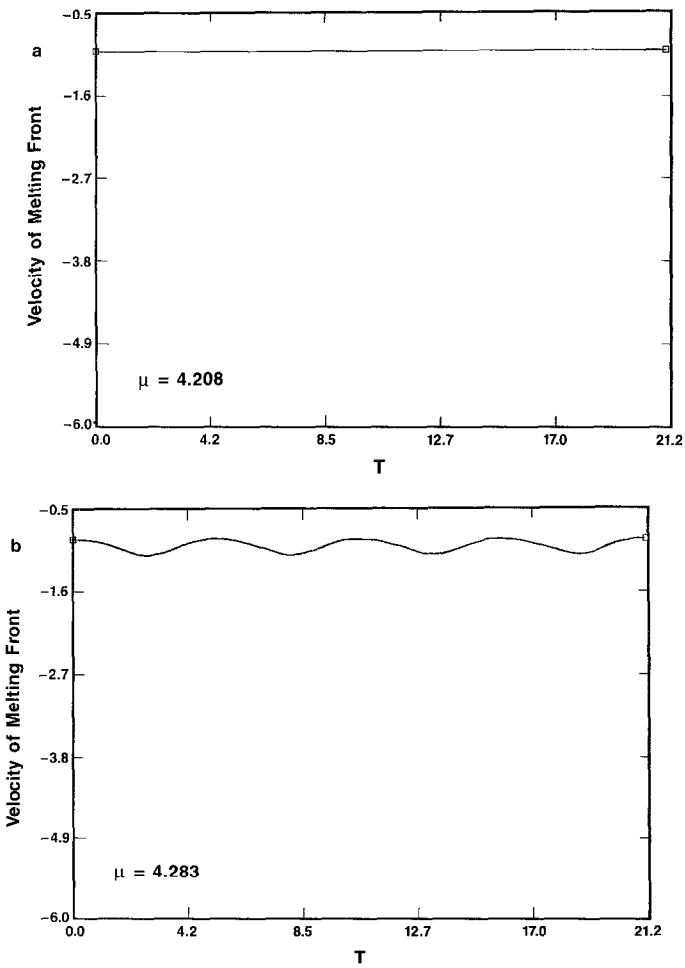

FIG. 5. Velocity of the melting front for different values of μ: (a) $\mu = 4.208$; (b) $\mu = 4.283$; (c) $\mu = 4.294$; (d) $\mu = 4.368$; (e) $\mu = 4.454$; (f) $\mu = 4.459$; (g) $\mu = 4.460$.

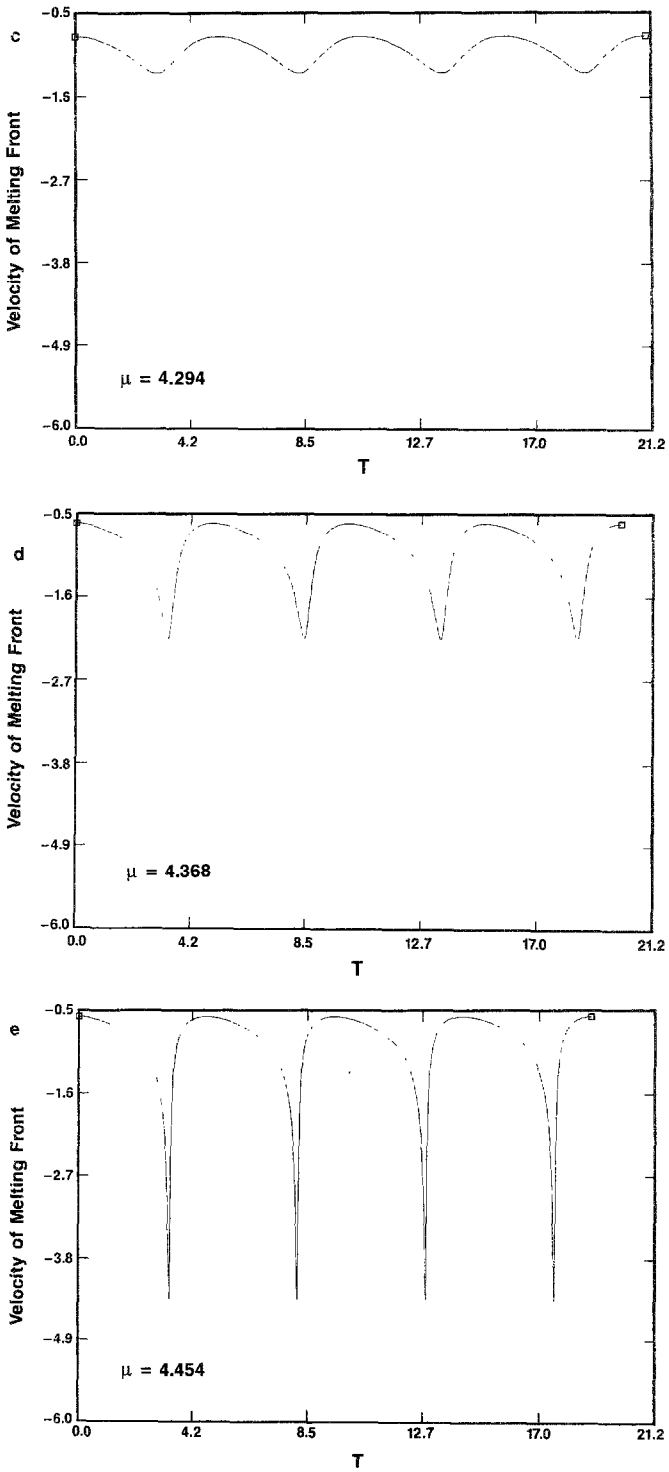

FIG. 5—*Continued*

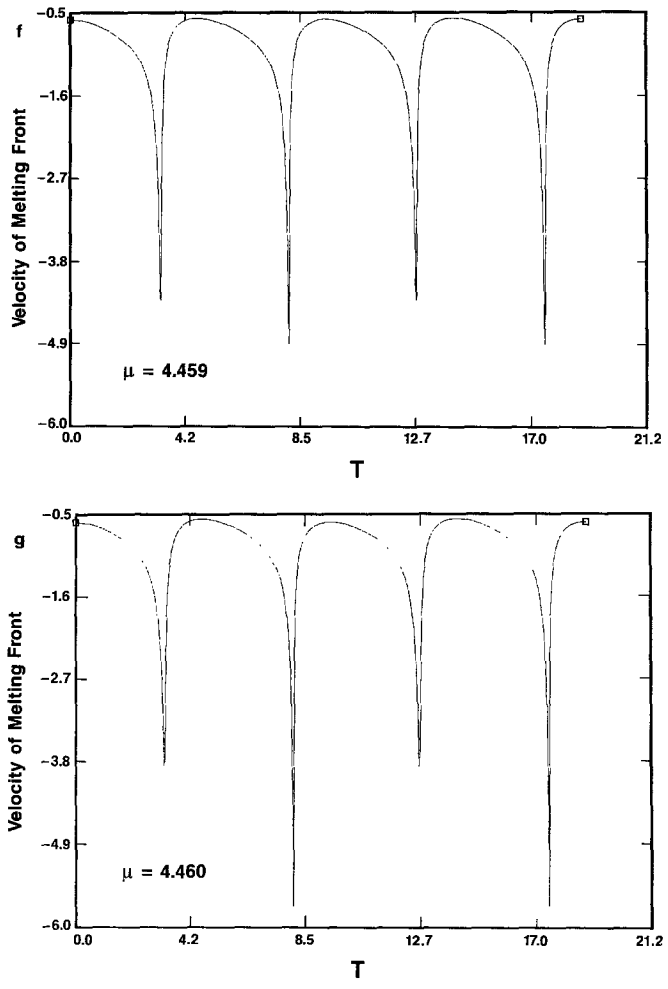

FIG. 5—*Continued*

cut-off location closer to (away from) the melting front, tends to increase (decrease) the amplitude of the spike. For all choices of cut offs that we have tested, the qualitative behavior of the solution, as μ increases, is the same. That is, the solution first exhibits a small amplitude sinusoidally oscillatory front, which develops into relaxation oscillations with progressively larger spikes and eventually into a period doubling bifurcation. In terms of the bifurcation diagram, with μ as the abcissa, changing z_c corresponds to a lateral shift. For any particular value of μ, however, the solutions for different z_c can differ markedly, since the amplitude of the oscillation is extremely sensitive to μ. In all cases the computational boundaries were chosen at $z_R = -z_L = 12$, and the results obtained were insensitive to increases of z_L or z_R.

In Figs. 5a–g we plot the computed velocity of the melting front, over four cycles, for values of μ ranging from 4.208 to 4.460. The corresponding range of σ is 0.8355 to 0.8250. We observe that stability is transferred from the steadily propagating front to the bifurcated oscillatory front for $\mu > \mu_1$, where μ_1 lies between 4.270 and 4.281. This compares well with the asymptotic *theoretical* prediction of 4.236 [14], which was computed for the case of infinite activation energy. The oscillations rapidly develop into relaxation oscillations with progressively sharper spikes of increasingly amplitude, as μ increases. Stability is then transferred at a period doubling secondary bifurcation point μ_2 which lies between 4.454 and 4.459. The growth of the larger spike is very rapid along the secondary branch. Since, in our method, we compute the solution of the initial boundary value problem and wait

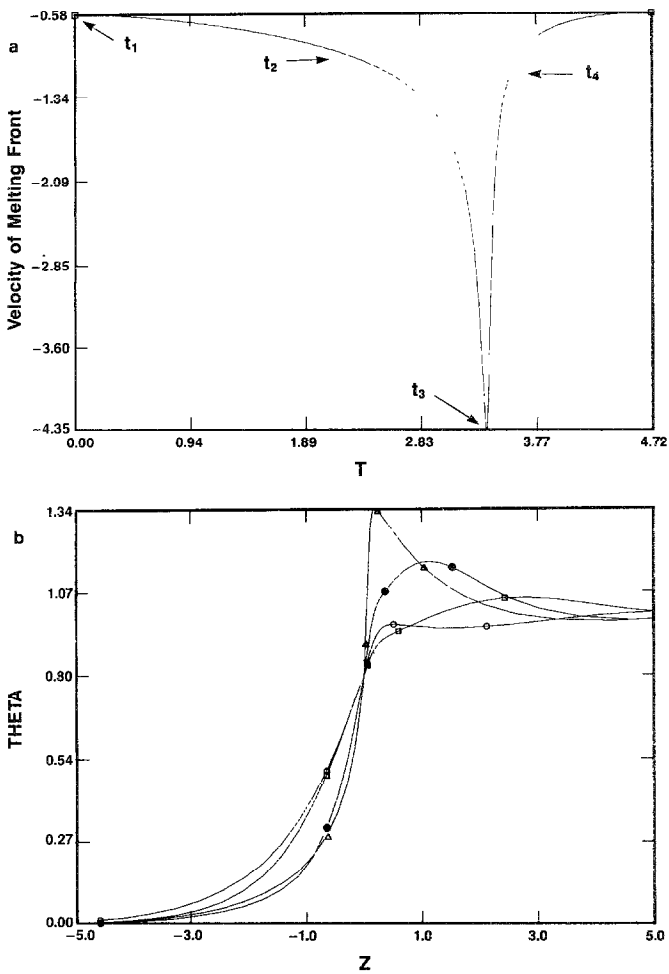

FIG. 6. (a) Velocity of the melting front plotted over one period $\mu = 4.454$. (b) Temperature profiles, $\theta(z)$, at selected times, $\mu = 4.454$. □, $t = t_1$; ○, $t = t_2$; △, $t = t_3$; ●, $t = t_4$.

until it eventually equilibrates to its stable steady state, we necessarily compute only the stable branches of the bifurcation diagram. It is therefore difficult in general to identify the fact that a bifurcation has occurred. Our reasons for claiming that secondary bifurcation has occurred are that (i) the equilibration times become much longer near this point, as they should on theoretical grounds, (ii) the character of the solution has changed dramatically at the point, abruptly doubling its period, and (iii) the difference in the amplitudes of the larger and smaller spikes goes to zero, as μ is decreased toward this point, as it should when a bifurcation point is approached from above.

In Fig. 6a we show the front velocity, plotted over one period, for $\mu = 4.454$. In

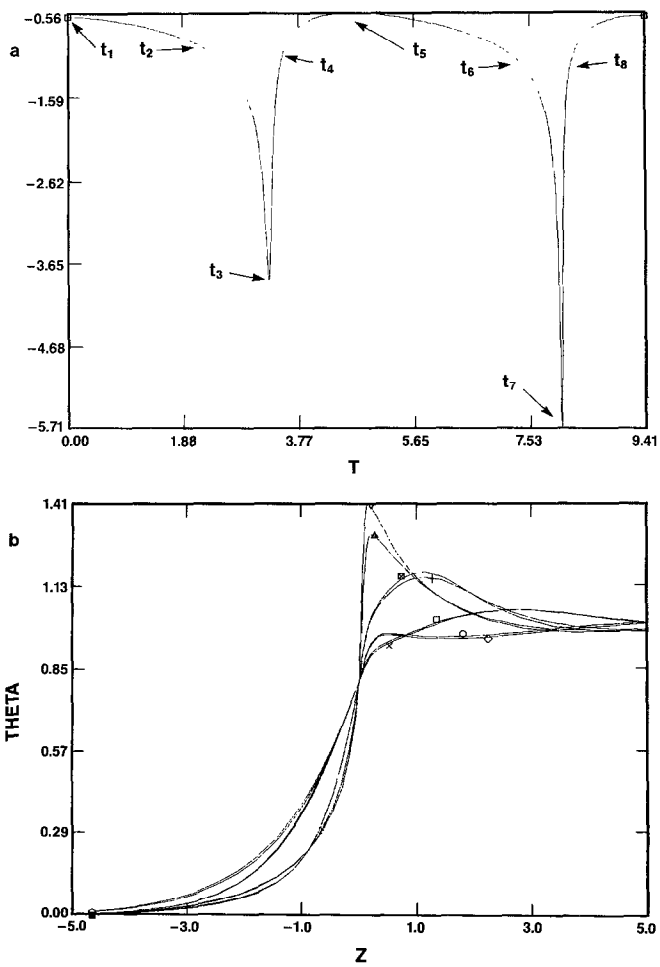

FIG. 7. Velocity of the melting front plotted over one period, $\mu = 4.460$. (b) Temperature profiles. $\theta(z)$, at selected times, $\mu = 4.460$. □, $t = t_1$; ○, $t = t_2$; △, $t = t_3$; +, $t = t_4$; ×, $t = t_5$; ◇, $t = t_6$; ▽, $t = t_7$; ⊠, $t = t_8$.

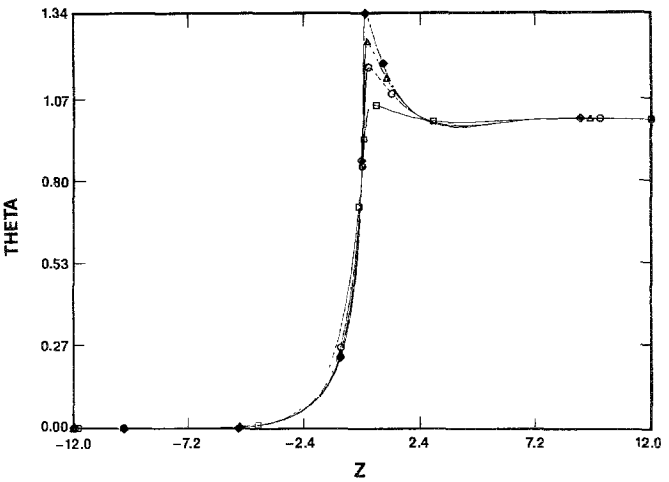

FIG. 8. Temperature profile, $\theta(z)$, for four different values of μ, at the instant that the velocity of the melting front spikes. □, $\mu = 4.294$; ○, $\mu = 4.368$; △, $\mu = 4.417$; ◆, $\mu = 4.454$

Fig. 6b we show the temperature profile $\theta(z)$ at four different times $t_1,\ldots, t_4$, during the cycle, as indicated on Fig. 6a. This is very close to the onset of period doubling. In Fig. 7a we show the front velocity, plotted over one period, for $\mu = 4.460$. In Fig. 7b we show $\theta(z)$ at eight different times, as indicated on Fig. 7a. In both cases the temperature spikes near the melting front, and a wave propagates outward toward $z = +\infty$. The wave is increasingly damped as z increases.

In Fig. 8 we plot the temperature profile $\theta(z)$ for four different values of μ, at the time of the spike. The profiles are all similar except for the amplitude and sharpness

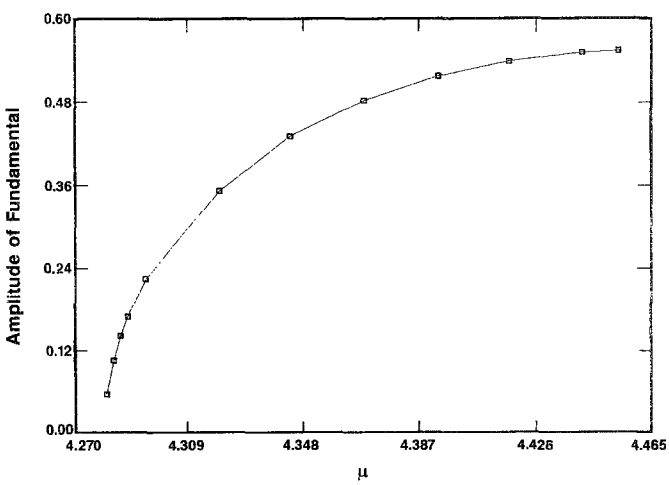

FIG. 9. Amplitude of fundamental obtained from Fourier analyzing melting front velocity over one period.

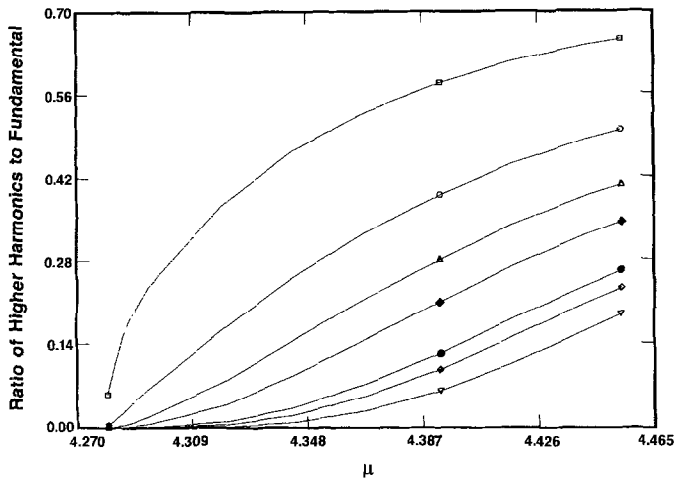

FIG. 10. Ratio higher harmonics to fundamental. □, first harmonic; ○, second harmonic; △, third harmonic; ◆, fourth harmonic; ●, sixth harmonic; ◇, seventh harmonic, ▽, tenth harmonic.

of the spike. We have Fourier analyzed the melting front velocity for values of μ beyond the first bifurcation point. In Fig. 9 we plot the amplitude of the fundamental as a function of μ. The nearly vertical behavior near the bifurcation point is characteristic of the supercritical behavior of the Hopf bifurcation (see, e.g., [5]). The fundamental saturates as μ increases. In Fig. 10 we plot the ratio of certain harmonics to the fundamental, again as a function of μ. The behavior of the different curves near the bifurcation point is again characteristic of supercritical behavior. The growth of the higher harmonics as μ increases is characteristic of relaxation oscillations.

5. CONCLUSION

We have exhibited the behavior of the solution as the bifurcation parameter μ increases. The velocity of the front evolves from steady to oscillatory as μ passes through the primary bifurcation point. The sinusoidal oscillations which occur very near the bifurcation point develop into relaxation oscillations, characterized by progressively sharper and narrower peaks. As a secondary bifurcation point is exceeded, a period doubling bifurcation is observed to occur.

We remark that though there is an actual front, the melting front, in this problem, most of the action does not occur at this front, but rather behind the front, in a region where the reaction term is most important. The width of this reaction zone is inversely proportional to the activation energy, which is typically large for combustion problems. Indeed, most of the prior analytical work corresponds to an asymptotic analysis for large activation energy, so that the reaction zone is a narrow layer which in the limit collapses to a moving surface, termed the reaction

"front." Thus, in this limit the distributed reaction is replaced by a localized reaction or heat source on this front, the strength of which is computed by the method of matched asymptotic expansions by constructing separate expansions within and outside of the reaction zone. Of course, for finite activation energies, such as are considered in this paper, there is no reaction front proper, and the actual Arrhenius reaction term is employed. Nevertheless, since the activation energy is large, though finite, the solution exhibits "front like" behavior in the reaction zone. This can be clearly seen in Figs. 6b, 7b, and 8. Our adaptive pseudo-spectral method is effective in correctly resolving this behavior.

Our results were obtained with an adaptive pseudo-spectral method, in which a new coordinate system is chosen to minimize a functional I, which is a Sobolev-type semi-norm of the solution, in that coordinate system. The effect of the method is to redistribute the collocation points so that the spectral interpolant better represents the solution. In our method we have employed a fixed number of collocation points, which are distributed according to the adaptive algorithm. The method can be modified to adaptively add and remove collocation points according to the size of I. In subsequent publications we plan to adaptively add or subtract points in considering both gasless and gaseous combustion problems, in both one and higher dimensions.

ACKNOWLEDGMENTS

The authors are grateful to E. Turkel for a useful discussion of the problem and to B. J. LeMesurier for his help with some of the computations.

REFERENCES

1. A. G. MERZHANOV, A. K. FILONENKO, AND I. P. BOROVINSKAYA, *Dokl. Phys. Chem.* **208**, 122 (1973).
2. YU. M. MAKSIMOV, A. T. PAK, G. B. LAVRENCHUK, S. YU. NAIBORODENKO, AND A. G. MERZHANOV, *Combustion Explosion and Shock Waves* **15**, 415 (1979).
3. YU. M. MAKSIMOV, A. G. MERZHANOV, A. T. PAK, AND M. N. KUCHKIN, *Combustion Explosion and Shock Waves* **17**, 393 (1981).
4. A. V. DVORYANKIN, A. G. STRUNIA, AND A. G. MERZHANOV, *Combustion Explosion and Shock Waves* **18**, 134 (1982).
5. B. J. MATKOWSKY AND G. I. SIVLASHINSKY, *S.I.A.M. J. Appl. Math.* **35**, 456 (1978).
6. D. GOTTLIEB AND S. A. ORSZAG. *C.B.M.S.-N.S.F. Regional Conference Series in Applied Mathematics No. 26*, S.I.A.M., Philadelphia, 1977.
7. E. J. DOEDEL AND R. F. HEINEMANN, *Chem. Eng. Sci.* **38**, 1493 (1983).
8. E. J. DOEDEL, in *Mathematical Methods in Energy Research: Proc. Special Year in Energy Math., U. Wyoming 1984*, edited by K. I. Gross (S.I.A.M., Philadelphia 1984), p. 103.
9. H. B. KELLER, in *Applications of Bifurcation Theory: Proceedings of an Advanced Seminar, Madison, Wisconsin, 1976*, edited by P. H. Rabinowitz (Academic Press, New York, 1977), p. 359.
10. B. ROGG, in *Notes on Numerical Fluid Mechanics 6: Proceedings of a GAMM Workshop, Aachen, W. Germany, 1981*, edited by N. Peters and J. Warnatz (Vieweg, Braunschweig/Weisbaden, 1982), p. 38.

11. M. D. Smooke and M. L. Koszykowski, *S.I.A.M. J. Sci. Stat. Computing*, **7**, 301 (1986).
12. S. B. Margolis, *Combin. Sci. and Tech.* **22**, 143 (1980).
13. S. M. Baer and T. Erneux, *S.I.A.M. J. Appl. Math.* **46**, 721 (1986).
14. S. B. Margolis, *S.I.A.M. J. Appl. Math.* **43**, 351 (1983).
16. C. Canuto and A. Quarteroni, *Math. Comput.* **38**, 67 (1982).
17. C. Canuto and A. Quarteroni, *S.I.A.M. J. Numer. Anal.* **19**, 629 (1982).
18. M. R. Malik, T. A. Zang, and M. Y. Hussaini, *J. Comput. Phys.* **61**, 64 (1985).